CHAPTER IV

RESULTS AND DISCUSSION

1. Isolation of Glabridin (4) from Licorice Extract.

Glabridin was an isoflavan which possessed extremely potent tyrosinase inhibitor. In this investigation, glabridin was isolated from licorice extract as a starting material. The isolation data of glabridin isolated from licorice extract (13.014 g) were summarized in Table 5.

Table 5. Isolation data of glabridin (4) isolated from licorice extract.

| Fraction No.	Weight of fraction (g)	% Tyrosinase inhibition	Weight of compound (4) (g)
F02	6.412	62	3.0303
F03	1.272	40	0.5021
F04	1.720	16	0.2300
Total			3.7624
			(28.91% yield of licorice extract)

The compound **4** was obtained as a white crystal. A molecular formular of $C_{20}H_{20}O_4$ was deduced from its [M + H]+ ion at m/z 325.1439 (calculated for $C_{20}H_{20}O_4$ + H, 325.1440) in the HRMS. The IR spectrum showed the presence of aromatic and olefinic structures (1607-1480) with phenolic hydroxyl group (3528-3351).

The 1H-NMR spectrum of **4** displayed a two methyl proton signal at δ 1.33 (H-5″ and H-6″). The aliphatic proton signals at δ 2.69 (d, J = 15.5, 4.2 Hz), 2.88 (dd, J = 15.5, 10.2 Hz) 3.29 (m), 3.92 (dd, J = 10.2, 10.2 Hz) and 4.23 (d, J = 10.2 Hz),

assignable to H-4eq, H-4ax, H-3ax, H-2ax and H-2eq, respectively. Two pair of olefinic protons with *ortho*-coupling (δ 5.63 and 6.53, each d, 1H, J = 9.9 Hz, H-3" and H-4"; δ 6.27 and 6.84, each d, J = 8.2 Hz, H-6 and H-5) were also observed. Moreover, the ^{1}H-NMR spectrum showed the presence of an ABM spin system at δ 6.18 (dd, J = 8.2, 1.3 Hz), 6.32 (d, J = 1.3 Hz) and 6.81(d, J = 8.2 Hz) should be assigned to H-5', H-3' and H-6', respectively. This was confirmed by the correlation observation in the two dimensional ^{1}H-^{1}H COSY spectrum (Figure 24). In addition, the downfield region of ^{1}H-NMR spectrum revealed the presence of two phenolic hydroxyl protons at δ 9.08 and 9.35.

The oxygen connected sp^3 carbon at δ 69.85 was assigned to C-2. With the aid of HMQC spectrum (Figure 25), the other protonated carbons could be assigned as summarized in Table 6. The assignment of quaternary carbons of compound **4** were made from the HMBC spectrum (Figure 26) as well as their chemical shifts.

Based on the spectral data described above as well as comparison with those of earlier reported ^{1}H and^{13}C NMR data (Kinoshita *et al.*, 1996a), the compound **4** was identified as glabridin.
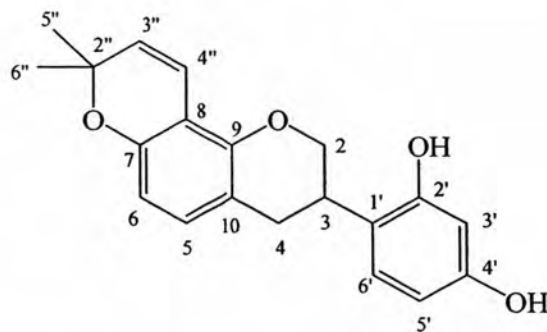
glabridin (**4**)

Table 6. NMR Spectral data of compound (4) and glabridin

| Position	Compound (4) in DMSO-d$_6$		Glabridin in CDCl$_3$	
	^{1}H (mult., J in Hz)	^{13}C	^{1}H (mult., J in Hz)	^{13}C
2ax	3.92(dd, 10.2, 10.2)	69.85	4.01 (dd, 10.3, 10.3)	70.0
2eq	4.23 (br d, 10.2)		4.39 (ddd,1.8, 3.2, 10.3)	
3ax	3.29 (m)	31.01	3.52 (m)	31.7
4ax	2.88 (dd, 15.6, 10.2)	30.09	2.99 (dd, 11, 15.7)	30.6
4eq	2.69 (dd, 15.5, 4.2)		2.83 (ddd, 1.8, 5.3, 15.7)	
5	6.84 (d, 8.2)	129.44	6.81 (d, 8.2)	129.2
6	6.27 (d, 8.2)	108.21	6.33 (d, 8.2)	108.7
7	-	151.34	-	151.9
8	-	109.15	-	109.9
9	-	149.36	-	149.8
10	-	114.841	-	114.3
1'	-	117.59	-	120.0
2'	-	155.96	-	154.4
3'	6.32 (d, 1.3)	102.64	6.46 (d, 2.2)	103.1
4'	-	156.98	-	155.2
5'	6.18 (dd, 8.3, 1.3)	106.42	6.39 (dd, 8.2, 2.2)	108.0
6'	6.81 (d, 8.2)	127.68	6.91 (d, 8.2)	128.4
2"	-	75.33	-	75.6
3"	5.63 (d, 9.9)	129.31	5.55 (d, 9.9)	128.9
4"	6.53 (d, 9.9)	116.53	6.64 (d,9.9)	116.9
5", 6"	1.33 (3H x 2, s)	27.33, 27.45	1.42 (s), 1.40 (s)	27.6, 27.8
2',4'-OH	9.08 (br s), 9.35 (br s)	-	7.48 (br s), 7.68 (br s)	-

2. Structural Modification of Glabridin.

2.1. Preparation of glabridin acyl ester derivatives.

The main problem of glabridin (4) in commercial products has been previously reported as poor skin penetration and instability in formulations (Nerya *et al.*, 2003). As known, the prodrug approach is one method of enhancing the activity of the drug by increasing its penetration rate through skin. In addition, the low stability of grabridin (4) may be caused by the oxidation reaction of phenolic hydroxyl moieties which can be protected by the acyl group. Therefore, acyl ester prodrugs preparation at phenolic hydroxyl groups of glabridin as well as their tyrosinase inhibitory and free radical scavenging activities are investigated in this study.

The two phenolic hydroxyl groups of glabridin can be easily transformed to diacyl ester derivatives (16-20), with various acid anhydrides in pyridine at room temperature as shown in Scheme 2. The proposed reaction mechanism of esterification was demonstrated in Scheme 3.

$R = COCH_3$, $CO(CH_2)_4CH_3$, $CO(CH_2)_8CH_3$,
$CO(CH_2)_{12}CH_3$, $CO(CH_2)_{16}CH_3$
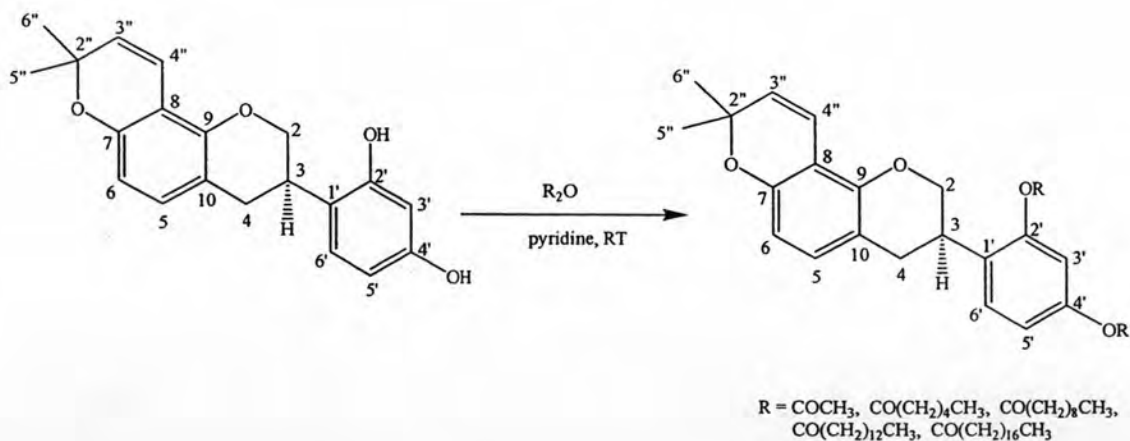
Scheme 2. Preparation of acyl ester derivatives of glabridin.
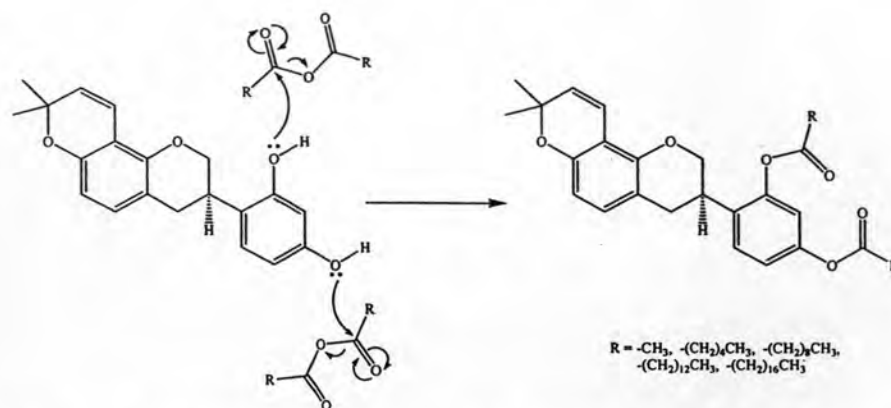
Scheme 3. The proposed reaction mechanism of esterification *via* acid anhydrides.

The structure of these derivatives were elucidated by extensive analysis of the spectroscopic data, mainly NMR spectra which showed the most characteristic signals similar to those of glabridin. All of the ^{1}H-NMR spectra of acyl groups at 2'-OH and 4'-OH displayed the similar proton signals except the carbonyl-connected methyl groups of glabridin acetate (**16**) were appeared at δ 2.30 and 2.27. The general structures and proton assignments of these derivatives are summarized in Figure 14. In addition, the ^{13}C-NMR revealed the presence of two carbonyl carbon at δ 179.02 and 172.06. The two carbon signals of C2' and C4' were shifted upfield and the carbon signals of C1', C3' and C5' were shifted downfield, while the other carbon signals were similar to those of glabridin. The structures and some physical properties of acyl derivatives (**16-20**) were summarized in Table 7.
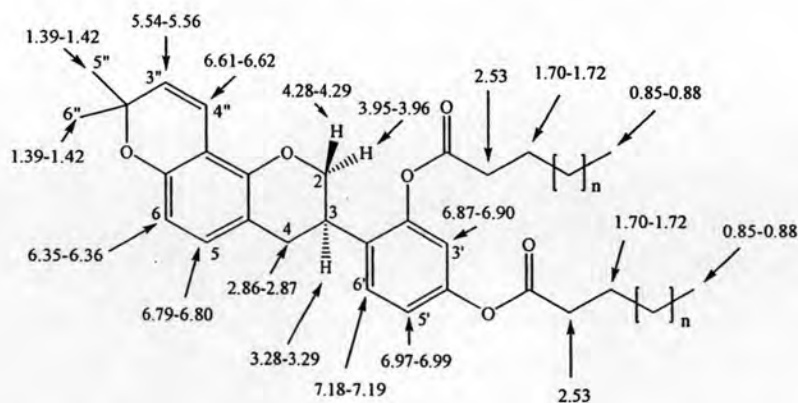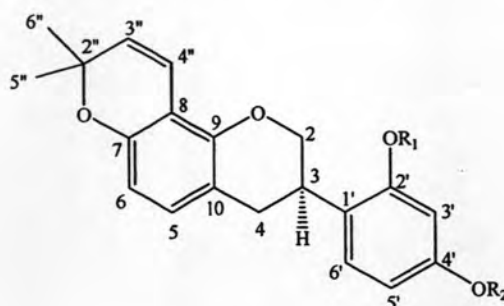

Figure 14. The general structures and proton assignments of compound **16-20**.

64

Table 7. The structures and some physical properties of compound **16-20**.

Compound	$R_1 = R_2$	Description	% Yield	Elemental analysis		Melting point (°C)
					C H	
16	acetyl	colorless crystal	97.35	calcd	70.57 5.92	177-179
				found	70.60 5.86	
17	hexanoyl	pale yellow oil	95.60	calcd	73.82 7.74	-
				found	73.85 7.69	
18	decanoyl	transparent oil	86.39	calcd	75.91 8.92	-
				found	75.06 8.78	
19	palmityl	white wax	84.58	calcd	77.95 10.06	37-38
				found	78.03 10.17	
20	stearyl	white wax	70.82	calcd	78.46 10.35	44-45
				found	78.45 10.35	

2.2. Preparation of 3″,4″-dihydroglabridin (21).

In order to investigate the role of the double bond between carbon atom 3″ and 4″ of glabridin (**4**), compound **21** has been designed and synthesized. Compound **21** was obtained from hydrogenation reaction of glabridin (**4**) as a pink-brown plate. The high resolution mass spectroscopy revealed *m/z* at 327.1589 (327.1596 calculated for $C_{20}H_{22}O_4 + H$).

According to ^{1}H-NMR,^{13}C-NMR, DEPT and HMQC spectra (Figure 62-66), compound **21** had 2 pairs of methylene protons at δ 1.69 (H-3″) and 2.50 (H-4″), in stead of two vinylic protons as seen in glabridin (**4**), while the other proton signals were similar to those of glabridin (**4**). In addition, the ^{13}C-NMR spectrum displayed the presence of two methylene carbons at 16.89 and 31.79 (C4″ and C3″), but two vinylic carbon signals as seen in glabridin (**4**), were disappeared.
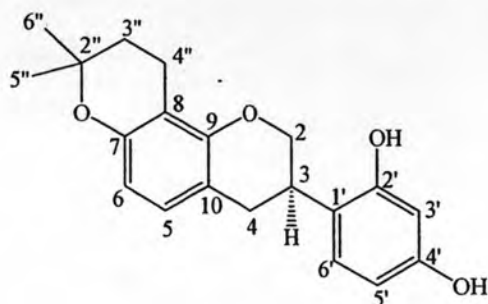

3″,4″-dihydroglabridin (**21**)

2.3. Preparation of glabridin benzoate analogues

Due to the lipophilic pocket surrounding tyrosinase active site, a number of benzoyl ester derivatives (**22-28**) of glabridin were synthesized. The benzoyl moiety may cause hydrophobic interaction with hydrophobic part of the enzyme. Thus the benzoyl esters were prepared with corresponding benzoyl chloride in pyridine at room temperature. The preparative scheme of benzoyl ester derivatives was shown in Scheme 4 and the proposed reaction mechanism was demonstrated in Scheme 5.
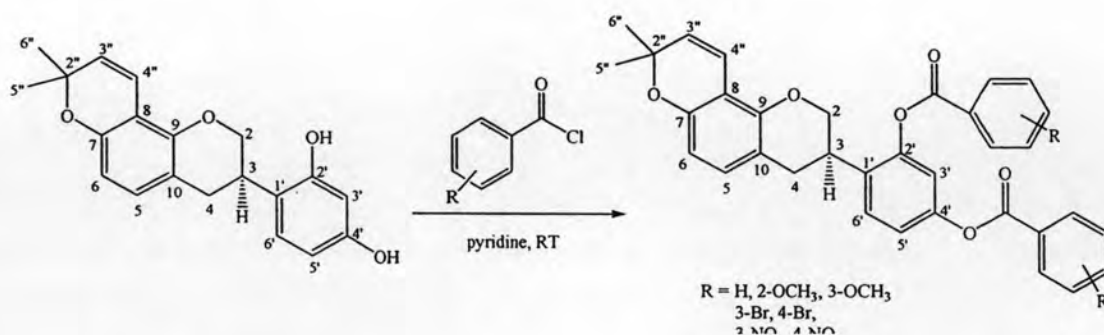
Scheme 4. Preparation of benzoyl ester derivatives of glabridin.
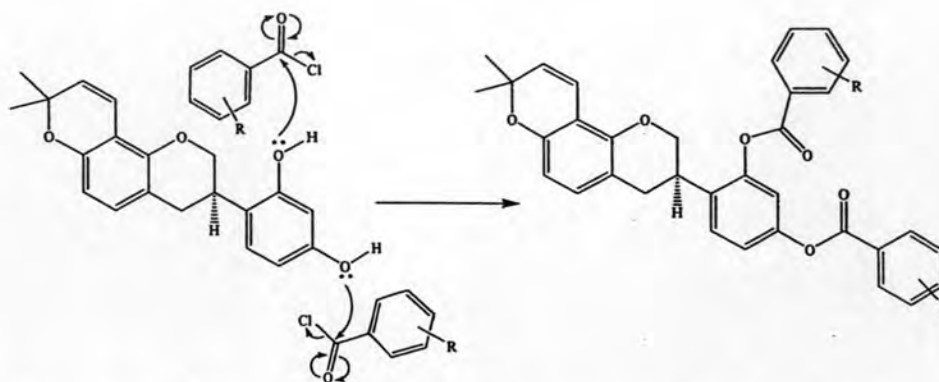
Scheme 5. The proposed reaction mechanism of esterification *via* acid chlorides.

The structures of the synthesized glabridin benzoate derivatives were elucidated predominantly by the interpretation of NMR , MS and elemental analysis data. The assignments for all protons and carbons of these compounds were mainly accomplished by extensive analyses through 1D-NMR and 2D-NMR measurements, including COSY and HMQC techniques. The most characteristic proton and carbon signals were similar to those of glabridin acyl esters, while the NMR data of the benzoyl and substituted benzoyl groups were summarized in Table 8. The ^{1}H-NMR signals displayed olefinic proton signals in the range of 7.17-9.01 ppm and ^{13}C-NMR signals in the range of 120.23–164.97 ppm. The structures and some properties of compound **22-28** were summarized in Table 9.

Table 8. ^{1}H-NMR and ^{13}C-NMR spectral data of benzoyl and substituted benzoyl groups of glabridin benzoate derivatives (**22-28**).

Compound	Substituent	NMR assignments	
		^{1}H (δ)	^{13}C (δ)
22		7.49 (4H, br t, J = 7.6 Hz), 7.62 (2H, br t, J = 7.6 Hz), 8.17 (4H, d, J = 7.6 Hz).	128.62 (2C), 128.76 (2C), 129.23 (2C), 130.22 (2C), 130.30 (2C), 133.75, 133.96,

Table 8. ^{1}H-NMR and ^{13}C-NMR spectral data of benzoyl and substituted benzoyl groups of glabridin benzoate derivatives (**22-28**) (continued).

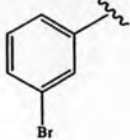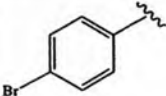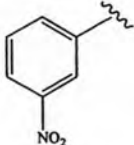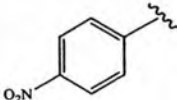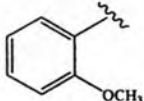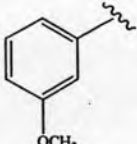| Compound	Substituent	NMR assignments	
		^{1}H (δ)	^{13}C (δ)
23		7.38 (2H, t, J = 8.0 Hz), 7.75 (2H, d, J = 8.0 Hz), 8.10 (2H, d, J = 8.0 Hz), 8.30 (2H, d, J = 1.5 Hz)	122.71, 122.85, 128.77, 128.82, 130.27, 130.33, 130.65, 131.09, 133.20, 133.25, 136.76, 136.98,
24		7.64 (4H, d, J = 8.4 Hz), 8.02 (4H, d, J = 8.4 Hz)	129.39 (2C), 131.48 (2C), 131.66 (2C), 131.72 (2C), 132.04 (2C), 132.19(2C)
25		7.73 (2H, t, J = 8.0 Hz), 8.5 (4H, br d, J = 8 Hz), 9.01 (2H, br s)	125.15, 125.30, 128.44, 128.53, 130.00, 130.15, 130.46, 130.94, 137.76 (2C), 149.43, 149.55,
26		8.35 (8H, s)	123.72, 123.76, 123.82, 123.96, 131.11, 131.29, 131.35, 131.45, 133.97, 134.44, 151.09, 151.18,
27		3.82 (3H, s, OCH$_3$), 3.92 (3H, s, OCH$_3$), 7.01 (4H, m), 7.52 (2H, m), 7.96 (2H, dd J = 7.5, 1.3 Hz),	55.76, 56.25, 112.07, 112.26, 118.87, 118.92, 120.23, 120.31, 132.18, 132.26, 134.39, 134.43, 159.58, 159.98
28		3.84 (3H, s, OCH$_3$), 3.86 (3H, s, OCH$_3$), 7.16-7.31 (2H, m), 7.40 (2H, td, J = 7.3, 1.1 Hz), 7.67 (2H, br s), 7.77 (2H, br d, J = 7.3 Hz)	55.52 (2C), 114.51 (2C), 120.40, 120.69, 122.65, 122.72, 129.65, 129.79, 130.08, 130.49, 159.74, 159.80

Table 9. The structures and some properties of compound **22-28**.
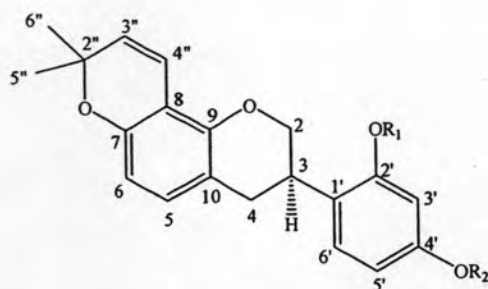
Compound	$R_1 = R_2$	Description	% Yield	TOF-MS (m/z)	Elemental analysis C H N
22	benzoyl	white wax	89.47	555.1798[M+Na]$^+$, calcd for $C_{34}H_{28}O_6Na$ 555.1778	calcd 76.69 5.26 found 76.62 5.30
23	m-bromo benzoyl	off-white wax	100	-	-
24	p-bromo benzoyl	white wax	61.03	-	-
25	m-nitro benzoyl	yellow crystal	60.37	645.1492[M+Na]$^+$, calcd for $C_{34}H_{26}N_2O_{10}Na$ 645.1480	calcd 65.59 4.18 4.50 found 65.58 4.20 4.55
26	p-nitro benzoyl	yellow amorphous	43.86	645.1488[M+Na]$^+$, calcd for $C_{34}H_{26}N_2O_{10}Na$ 645.1480	calcd 65.59 4.18 4.50 found 65.64 4.19 4.53
27	o-methoxy benzoyl	white bulky powder	63.75	-	calcd 71.83 5.63 found 71.82 5.65
28	m-methoxy benzoyl	white bulky powder	86.02	-	calcd 71.83 5.63 found 71.80 5.67

3. Determination of Tyrosinase Inhibitory Activity.

Since tyrosinase is the important key enzyme in melanin biosynthesis in plants and animals as well as in insect molting. Tyrosinase inhibitors have recently been interesting compounds due to decreasing or inhibition the enzyme action. They are supposed to have broad applications in medicinal and cosmetic products. Many efforts have been spent in the search for feasible and effective tyrosinase inhibitors, particularly from plants (Shi *et al.*, 2005). In this present study, Glabridin (**4**) has been isolated from licorice extract as a precursor and the structure activity relationship of the modified compounds on tyrosinase inhibition was studied.

The tyrosinase inhibitory activity of each modified compound was determined by the dopachrome method, which was adapted from the procedure described by Iida (Iida *et al.*, 1995), Shin (Shin *et al.*, 1998). and Likhitayawuid and Sritularak (Likhitayawuid and Sritularak, 2001). All of the glabridin derivatives prepared in this study were evaluated for tyrosinase inhibitory activity initially at the concentration of 0.33 mg/ml, using kojic acid as positive control. It was found that only glabridin (**4**) and 3″,4″-dihydroglabridin (**21**) exhibited more than 50% inhibition, and therefore the compounds were further analyzed to determine the IC_{50} values. It should be noted that, glabridin (**4**) was earlier reported as a stronger tyrosinase inhibitor than kojic acid, a well known tyrosinase inhibitor and it was confirmed in this experiment, as demonstrated IC_{50} values of 18.58 and 147.58 μM, respectively.

As previously mentioned, the hydrophobic pocket surrounding the binuclear copper active site of tyrosinase enzyme was also important for inhibitors to interact with the enzyme (Kubo *et al.*, 2003; Son *et al.*, 2006). Thus, a series of glabridin benzoate derivatives (**22-28**) have been designed and synthesized, but none of them exhibited significant inhibitory activity including acyl esters of glabridin (**16-20**). This results confirmed that the 4-substituted resorcinol skeleton was a pharmacophore requirement for tyrosinase inhibitory activity.

In order to investigate the role of the olefin structure, glabridin (**4**) with double bond between carbon atom 3″ and 4″ was reduced by hydrogenation reaction. The corresponding product, 3″,4″-dihydroglabridin (**21**) was exerted higher inhibitory

effect on tyrosinase activity (IC_{50} = 11.40 μM). Thus, the higher tyrosinase inhibitory activity of 3″,4″-dihydroglabridin (**21**) was probably due to the lacking of the double bond between carbon atom 3″ and 4″, which gave more flexibily and allowed the resorcinol groups to interact with the enzyme more effectively. Further analysis of data obtained for 3″,4″-dihydroglabridin (**21**) indicated that this compound, together with glabridin (**4**) and kojic acid (**2**), inhibited the enzyme in a dose-dependent manner as shown in Figure 15.

Tyrosinase inhibition
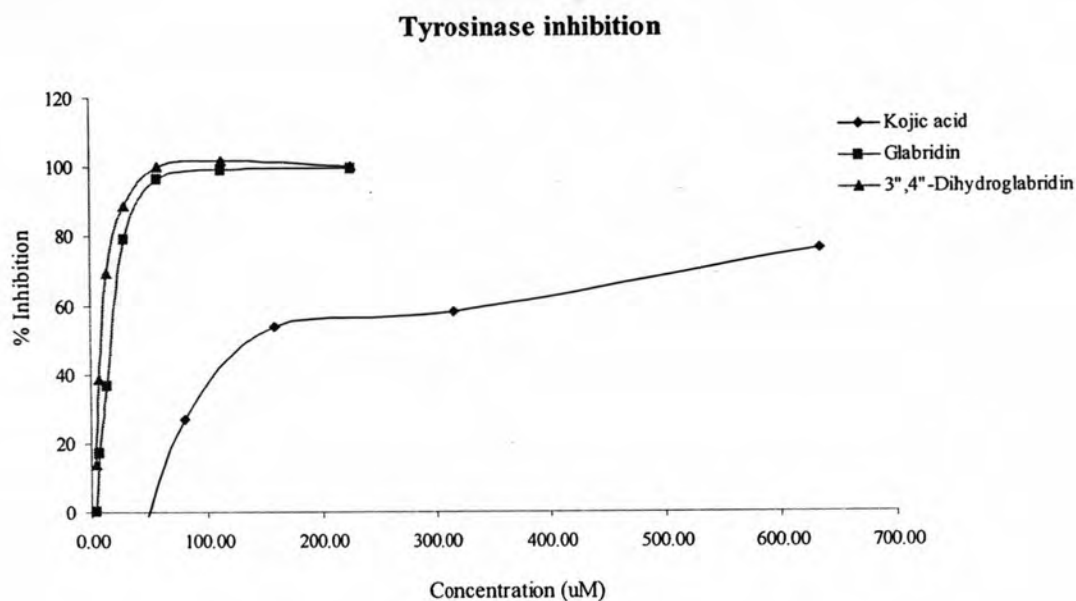

Figure 15 Dose-dependent inhibitory effects on mushroom tyrosinase by glabridin (**4**), 3″,4″-dihydroglabridin (**21**) and kojic acid (**2**).

The results of glabridin (**4**) and its analogues (**16-28**) on mushroom tyrosinase were illustrated as the percentage of tyrosinase inhibition and IC_{50} values in comparison with kojic acid (**2**), are summarized in Table 10.

Table 10. Tyrosinase inhibitory activity of glabridin and their derivatives.

Compounds	% Tyrosinase inhibition at 0.33 mg/ml[a]	IC$_{50}$ (μM)
Glabridin (4)	99.80	18.58
Glabridin diacetate (16)	-4.81	-
Glabridin dihexanote (17)	-9.02	-
Glabridin didecanoate (18)	-7.60	-
Glabridin dipalmitate (19)	-4.85	-
Glabridin distearate (20)	0.09	-
3″,4″-Dihydroglabridin (21)	100.00	11.40
Glabridin-2′,4′-O-dibenzoate (22)	-21.37	-
Glabridin-2′,4′-O-di-3‴-bromobenzoate (23)	-46.70	-
Glabridin-2′,4′-O-di-4‴-bromobenzoate (24)	-24.94	-
Glabridin-2′,4′-O-di-3‴-nitrobenzoate (25)	27.42	-
Glabridin-2′,4′-O-di-4‴-nitrobenzoate (26)	-1.76	-
Glabridin-2′,4′-O-di-2‴-methoxybenzoate (27)	22.50	-
Glabridin-2′,4′-O-di-3‴-methoxybenzoate (28)	-41.43	-
Kojic acid (2)	76.41	147.58

[a] compounds with more than 50% inhibition were further analyzed for IC$_{50}$ values.

4. Determination of Free Radical Scavenging Activity

The role of free radicals in many disease conditions has been well established. Several biochemical reactions in our body generate reactive oxygen species (ROS) which are capable of damaging crucial biomolecules and lead to disease conditions due to non-effectively scavenged by cellular constituents (Kumaran and Karunakaran, 2006). However, the harmful of free radicals can be blocked by antioxidant substance, which can interfere with oxidation process by reacting with free radicals, chelating free catalytic metals and also by acting as oxygen scavengers.

Since phenolic compounds was known to exert antioxidant properties, due to their ability to donate an electron or sometimes chelate metals. Antioxidant actitivity of phenolic compounds may also prevent or delay pigmentation resulting from auto-oxidation. In this investigation, the antioxidant activity of glabridin and its analogues was examined by measuring their ability to donate an electron to the free radical compound, DPPH. The DPPH assay is based on the reduction of methanolic DPPH solution (purple color) in the presence of a hydrogen-donating antioxidant lead to the formation of non-radical form DPPH-H (yellow color) (Son and Lewis, 2002). as shown in Figure 16.
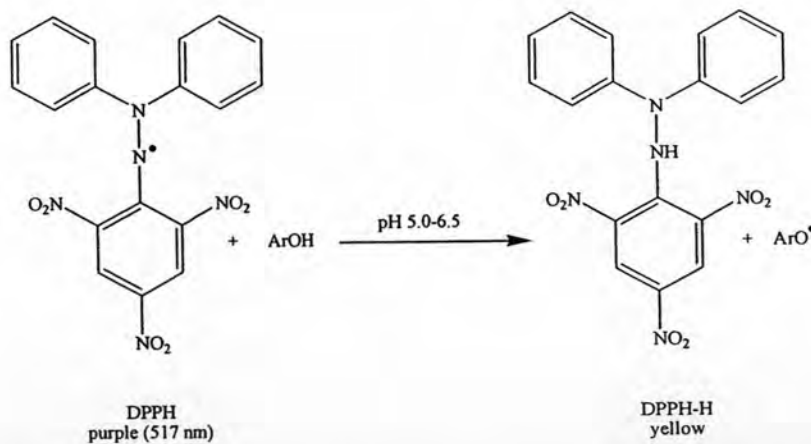

DPPH
purple (517 nm)

DPPH-H
yellow

Figure 16. Radical scavenging action of antioxidants (ArOH) (Son and Lewis, 2002).

According to the IC_{50} values displayed in Table 11, Glabridin (4) and 3″,4″-dihydroglabridin (21) were the only two compounds which showed free radical scavenging activities, but both of them were less efficient comparatively with the

positive control, quercetin. The structures of these active compounds were composed of free hydroxyl groups. As comparison with quercetin (**29**), glabridin (**4**) and 3″,4″-dihydroglabridin (**21**) contained only two free hydroxyl groups, thus they exhibited as mild free radical scavengers. This suggested that the free hydroxyl group should be important for the free radical scavenging activity. Like quercetin (**29**) glabridin (**4**) and 3″,4″-dihydroglabridin (**21**) scavenged the free radical in a dose-dependent manner (Figure 17).
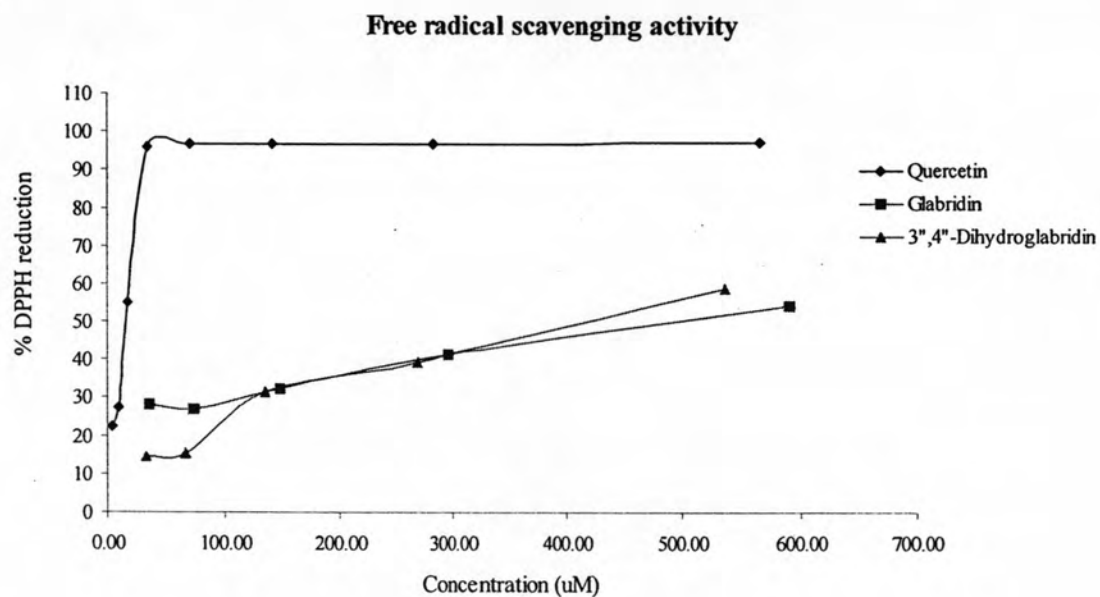
Free radical scavenging activity

Figure 17. Dose-dependent free radical scavenging activity of glabridin (**4**), 3″,4″-dihydroglabridin (**21**) and quercetin (**29**).

Table 11. Free radical scavenging activity of glabridin and their derivatives.

Compounds	% Scarvenging activity at 0.33 mg/ml[a]	IC$_{50}$ (μM)
Glabridin (4)	70.52	492.71
Glabridin diacetate (16)	6.55	-
Glabridin dihexanote (17)	5.96	-
Glabridin didecanoate (18)	5.60	-
Glabridin dipalmitate (19)	10.20	-
Glabridin distearate (20)	5.06	-
3″,4″-dihydroglabridin (21)	77.63	416.84
Glabridin-2′,4′-O-dibenzoate (22)	12.16	-
Glabridin-2′,4′-O-di-3‴-bromobenzoate (23)	3.51	-
Glabridin-2′,4′-O-di-4‴-bromobenzoate (24)	4.40	-
Glabridin-2′,4′-O-di-3‴-nitrobenzoate (25)	3.23	-
Glabridin-2′,4′-O-di-4‴-nitrobenzoate (26)	4.95	-
Glabridin-2′,4′-O-di-2‴-methoxybenzoate (27)	4.60	-
Glabridin-2′,4′-O-di-3‴-methoxybenzoate (28)	6.19	-
Quercetin (29)	96.19	16.15

[a] compounds with more than 50% inhibition were further analyzed for IC$_{50}$ values.

5. Determination of Partition Coeffient (log P)

The dermal drug transport is greatly limited by unsuitable physicochemical properties of most drugs and the efficient barrier function of the skin. Therefore, many efforts of improving topical drug absorption have been performed such as prodrug approach. The lipophilicity of the prodrug and its parent compound was determined as a partition coefficient. It has long been known that the n-octanol/water system is a good mimic of the water/membrane interface. The partition coefficient (log P) is evaluated by measuring the concentrations of a chosen species in both phases. Accordingly, log P has been extensively utilized to predict the relative tendency of compounds to interact or incorporate in biological membranes (Engelmann *et al.*, 2007). In this study, the partition coefficient of all prodrugs (**16-20**) was determined as comparison with their parent drug, glabridin (**4**) using n-octanol/phosphate buffer pH 5.5 system. The volume ratio of n-octanol and buffer phase was 1:10. The partition coefficient of glabridin and its prodrugs were summarized in Table 12.

Table 12. Partition coefficient of glabridin (**4**) and its prodrugs (**16-20**).

Compound	P_{app}	log P_{app}[a]
Glabridin (**4**)	61.391	1.79
Glabridin diacetate (**16**)	51.678	1.71
Glabridin dihexanote (**17**)	59.351	1.77
Glabridin didecanoate (**18**)	63.122	1.80
Glabridin dipalmitate (**19**)	71.688	1.86
Glabridin distearate (**20**)	179.068	2.25

[a]log P_{app} is partition coefficient between n-octanol and phosphate buffer pH 5.5 at room temperature.

The apparent partition coefficient of all prodrugs ranged from 1.71 to 2.25. Most of the prodrugs have higher log P values than their parent drug, except glabridin diacetate (16) and glabridin dihexanoate (17). The results obtained indicated that the partition coefficient of the prodrugs increased as the number of carbon atom in the aliphatic chain of the acyl moiety increased. Since the log P value was depended upon the solubility of the compound. Generally, molecules with high melting points showed strong intermolecular forces. Such molecules had little tendency to dissolve in the organic phase and consequently, their partitioning into the lipoidal barrier phase of the skin is minimal (Kim et al., 2005). In addition, the compound containing a long alkyl chain had poor solubility in the protic solvent such as n-octanol. Therefore, the lower log P values were resulting from the high melting point and the low capacity to dissolve. Thus, a proper vehicle to increase the solubility would be necessary in order to further increase the delivery of glabridin derivatives.

6. Enzymatic and Chemical Hydrolysis Studies

The precondition of prodrug approach is that the prodrug can be converted to the parent drug in order to exert biological effects. Thus evaluation of enzymatic and chemical hydrolysis of prodrug, glabridin diacetate (16) was performed. As porcine liver esterase is a good model of the esterase found in the skin and, as such, is important in predicting the use of certain prodrugs as topical treatment (Redden et al., 1999). In this investigation, the porcine esterase was used as a tool for enzymatic hydrolysis study of glabridin diacetate (16). The retention time in this HPLC system were: glabridin (4) 4.704 min, betamethasone valerate (IS) 5.269 min and glabridin diacetate (16) 7.756 min. It was shown that the porcine liver esterase can easily catalyze hydrolysis of phenol ester of glabridin diacetate (16) prodrug, lead to the release of its parent drug, glabridin (4). The hydrolysis of glabridin diacetate (16) was found to proceed in two step reaction. Firstly, one of the ester moiety was hydrolyzed to yield glabridin acetate which underwent spontaneous hydrolysis to glabridin as shown in Figure 18.
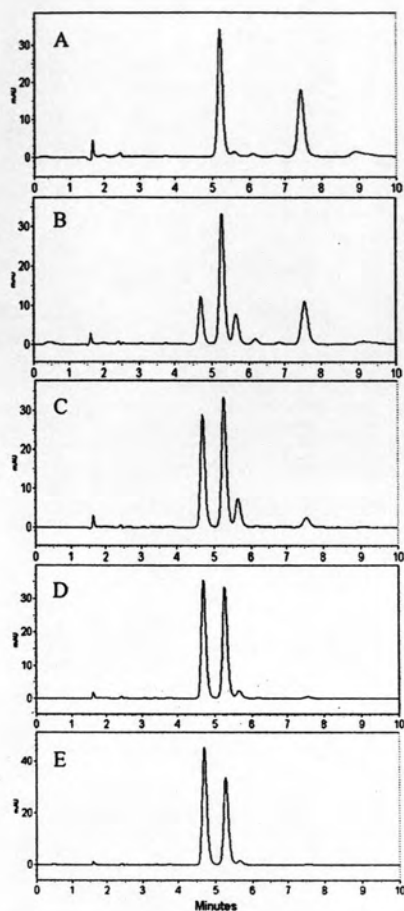
Figure 18. Typical HPLC chromatograms of glabridin diacetate (16). Panel A: starting material, panel B: 2 min after the addition of esterase, panel C: 6 min after the addition of esterase, panel D: 10 min after the addition of esterase, panel E: 120 min after the addition of esterase.
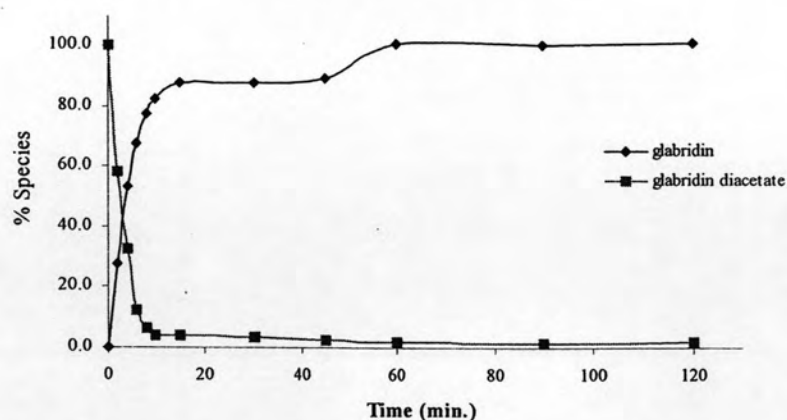
Enzyme hydrolysis

Figure 19. Time course for glabridin diacetate (16) prodrug and its hydrolysis product, glabridin (4) by porcine liver esterase.

The results from Figure 19 indicated that in the first 6 min, the rate of enzymatic hydrolysis of glabridin diacetate (16) prodrug was very fast and the time required to reach the steady state of hydrolysis was 10 min. The half-life of glabridin diacetate (16) in the presence of porcine liver esterase was 2.34 min, therefore, this prodrug may be more susceptible toward esterase catalytic hydrolysis due to the lack of steric hindrance.

The stability of prodrug against the spontaneous chemical hydrolysis is of importance, especially for the cosmetic products and topical drugs formulation. The chemical hydrolysis in this study was performed in phosphate buffer pH 5.5 and 7.4 at 37 °C to evaluate the effect of pH on degradation of glabridin diacetate (16) prodrug. The sign of chemical degradation of the test prodrug was seen after 24 h, however, the degradation rate was very slow as comparison with enzymatic hydrolysis. The result obtained indicated that the chemical stabilities of glabridin diacetate (16) prodrug at pH 5.5 and 7.4 were quite similar. The half-lives of hydrolysis in both pH buffer solution were more than 15 days, suggesting the sufficient chemical stability.
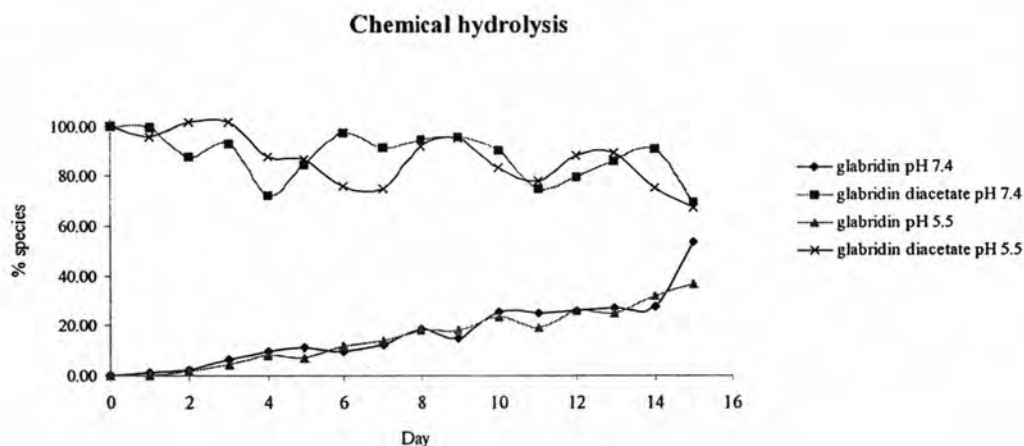

Figure 20. Time course for glabridin diacetate (16) prodrug and its hydrolysis product, glabridin (4) in phosphate buffer pH 5.5 and 7.4.